International Journal of Current Science Research and Review
ISSN: 2581-8341
Volume 06 Issue 12 December 2023
DOI: 10.47191/ijcsrr/V6-i12-99, Impact Factor: 6.789
IJCSRR @ 2023
www.ijcsrr.org

Global Stability Study of a Reinforced Concrete Building: Comparison between Grid and Space Frame Model with an Integrated Model

José Pedro Diniz Figueiredo[1], Leovegildo Douglas Pereira de Souza[2]
[1,2] Center for Agrifood Sciences and Technology, Federal University of Campina Grande, Pombal, Brazil

ABSTRACT: The verticalization in large urban centers has provided a series of new challenges for large buildings designers. The slender the structures are, more susceptible they are to second-order global efforts, making its verification indispensable for any reinforced concrete structure. As allies, technological advances and the processing power of computer systems have enabled greater productivity in the verification of the global stability of large buildings. Over the years, several structural models have been implemented in structural analysis and design, aiming to better simulate the actual behavior of structures. In view of this, the present work aims to perform a comparative analysis of the global stability of a reinforced concrete building, using the grid models associated with the space frame and the integrated model. Moreover, the research aims to verify the importance of the structural elements in the global stability of the building. In study two different structural systems were employed for the same building, verifying through the TQS *software* the conception that presents the best behavior according to the model used. Based on the results obtained, some guidelines are proposed regarding the use of structural models, indicating which one presents the best behavior according to the characteristics of the building.

KEYWORDS: Global stability, Reinforced concrete, Second-order effects, Structural models, Structural analysis

1. INTRODUCTION

Due to population growth and the need to improve the use of urban space, arise a tendency for verticalization of buildings in large cities of the country, through the construction of taller and slender structures. In tall buildings, wind loads and geometric imperfections are the main horizontal loads that, along with other loads, can cause additional stresses on the structure, called second-order effects. For these situations, the effects mentioned must be verified in the project, to ensure stability and good performance of the building throughout its life.

The second-order effects are inversely related to the global stability of buildings, so, the greater the second-order effects, the less stable is the structure. Some parameters are used to analyze the global stability of buildings, such as the α parameter, γz coefficient, and the P-Δ process. According to Bueno [1], these parameters are used to evaluate the structure's sensitivity and used by designers to analyze the need to consider or not the second order effects, still in the initial phase of the project.

Currently, due to technological advances, several computer systems are used in the design of reinforced concrete structures. According to Kimura [2], using software in structural design, as long as it is used responsibly and carefully, provides a higher level of productivity, quality, and safety to the project. Through the increase in the processing capacity of computer systems, it is possible to analyze the structure through structural models that simulate more closely the real behavior of the building.

Also, according to Kimura [2], several structural models can be applied to the analysis of reinforced concrete structures. Currently, one of the most used models by structural software is based on the combination of beam grid and slab model with the space frame. In this model, the slabs are dimensioned separately and the loads from the slabs on the beams are transferred to the space frame, performing a global analysis of the building and dimensioning the beams and pillars. Another commonly used model is the integrated model, where the slabs are analyzed together with the space frame and the whole structure behaves as a single body.

According to Moncayo [3], some design criteria such as the rigidity of the structure and the structural model used can directly affect the overall stability of a building. Thus, through the aid of structural software, this paper aims through two different structural conceptions, to perform a comparative analysis of the overall stability of a reinforced concrete building, using the parameters α, γz, and P-Δ, comparing the results obtained through the beam grid and slab models associated with the space frame and through the integrated model.

International Journal of Current Science Research and Review
ISSN: 2581-8341
Volume 06 Issue 12 December 2023
DOI: 10.47191/ijcsrr/V6-i12-99, Impact Factor: 6.789
IJCSRR @ 2023
www.ijcsrr.org

2. BIBLIOGRAPHIC REVIEW

2.1 Actions and combinations in buildings

The definition of loads and loads acting on a structure is a fundamental step for the correct design of a building. According to ABNT NBR 6118 [4], the structural analysis stage aims to survey the loads and active actions on a structure. Through the survey of loads and combinations, it is possible to obtain the efforts (normal and tangential) and the design of the elements, aiming to ensure the safety and functionality of the building, reducing the probability of ruin and providing acceptable conditions of use during its service life.

2.1.1 Limit states

The design of a structure should ensure the safety and functionality of the building during its entire service life. For this, a structure must meet the limit states that are classified as the ultimate limit state and service limit state. The first occurs when the structure collapses partially or totally and is directly related to its strength. The second occurs when the structure no longer meets the appropriate criteria for use due to its malfunction [2].

2.1.2 Actions in structures

All actions capable of producing significant stresses and strains in a building should be considered in the design of the elements of a structure. According to ABNT NBR 8681 [5], the active actions on a structure can be classified as permanent, variable, and exceptional.

2.1.2.1 Permanent actions

According to ABNT NBR 6118 [4] permanent actions are those whose values do not present great variations throughout the building's useful life and are classified as direct and indirect actions.

- Direct permanent actions are loads arising from the structure's weight, permanent construction elements, fixed equipment and facilities, non-removable soil thrust, and other permanent loads applied to the structure;
- Indirect permanent actions are loads originating from deformations imposed by concrete shrinkage and creep, support settlements due to displacement of structural elements, prestressing forces in prestressed concrete parts, and geometric imperfections.

2.1.2.2 Variable Actions

According to Araújo [6], the variable actions are those that loads undergo significant variations of their values over the structure’s life. These loads come from the weight of people, vehicles, furniture, wind effects, and temperature variations, among other variable loads existing in a building. In function of the probability of occurrence, the variable loads are classified as normal or special.

- Normal variable actions are those who have significant probabilities of occurrence, and it is mandatory to consider them when designing structures;
- Special variable actions are actions of seismic origin or accidental loads of a special nature, or intensity.

2.1.2.3 Exceptional actions

The exceptional loads are loads that have a short duration and a low probability of occurrence during the service life of the building. These actions come from fires, floods, explosions, or exceptional earthquakes, being necessary to be considered in the design of structures subject to these loads, where their effects cannot be controlled by other means [4].

2.1.3 Combinations of actions

According to Kimura [2], a real building will be subject to several actions simultaneously. The combination of actions acting on a reinforced concrete structure should be done so that the most unfavorable effects on the structure can be considered. According to ABNT NBR 6118 [4], the combinations can be classified into ultimate combinations and service combinations, which are used respectively for the verification of ultimate limit states and service limit states.

The ultimate combinations are used to define the internal forces that will be used in the design of the structural elements. An ultimate combination can be classified as normal, special or construction, and exceptional, the former being most commonly used in the calculation of reinforced concrete buildings.

International Journal of Current Science Research and Review
ISSN: 2581-8341
Volume 06 Issue 12 December 2023
DOI: 10.47191/ijcsrr/V6-i12-99, Impact Factor: 6.789
IJCSRR @ 2023
www.ijcsrr.org

The service combinations are used to verify deflections, cracks, and vibrations. A service combination can be classified as almost permanent, frequent, and rare, being the first two most commonly used in reinforced concrete buildings. The almost permanent combination can be used to verify the limits state of excessive deformations. The frequent combination can be used to verify the limit states of crack formation, crack opening, and excessive vibrations. Besides these, it can also be used to verify the limits state of excessive deformations, resulting from the action of wind or temperature.

2.1.4 Wind loads

According to Carmo [7], wind loads and geometric imperfections are the main causes of horizontal actions present in structures that must be considered in the analysis of building stability. The effects of wind load on buildings are directly related, among other factors, with their height, being one of the most important actions in structural design.

According to Gonçalves et al. [8], wind action on structures depends on meteorological and aerodynamic aspects. The first concerns the wind speed, being related to the location of the building, type, and roughness of the terrain, building height, and occupation. The aerodynamic aspect is related to the shape of the building due to the different behavior that the wind has according to its geometry.

To determine the forces exerted by the wind in reticulated structures, the actions can be considered as concentrated loads, applied at each slab level. Thus, it is necessary to determine the intensity of the loads acting on each frame of the structure, which varies according to its stiffness [9].

The consideration of the effects caused by wind loads on a structure is fundamental for the good performance of the building throughout its service life. The guidelines and orientations to consider wind loads on a building are established according to ABNT NBR 6123: 1988 - Forces due to wind on buildings [10].

2.2 Structural Analysis Models

Structural analysis is one of the most important stages of a structural project because it is from the results obtained that the dimensioning and detailing of structural elements are performed [2]. It is from the structural analysis stage that it is possible to perform a prediction of the building's behavior, verifying the internal efforts, displacements, and deformations on the structure after the application of loads.

According to ABNT NBR 6118, [4] structural analysis is performed from the definition of a structural model that aims to simulate the behavior of the real structure. "The creation of the structural model of a real structure is one of the most important tasks of structural analysis." [11].

There are several structural calculation software's in the market that allows the definition of the structural model that best fits the behavior of the real building. It's the designer's responsibility to define the most adequate model to analyze a structure inside a software. Currently, the structural analysis of reinforced concrete buildings is mainly based on the combination of beam grid and slab models with space frames [2].

2.2.1 Beam grid and slab model

According to Kimura [2], the grid model of beams and slabs, also known as grid analogy, is a structural model composed of bars in the horizontal plane that simulate the beams and slabs, forming a mesh subjected to vertical loads. This model is commonly used for the structural analysis of reinforced concrete floors.

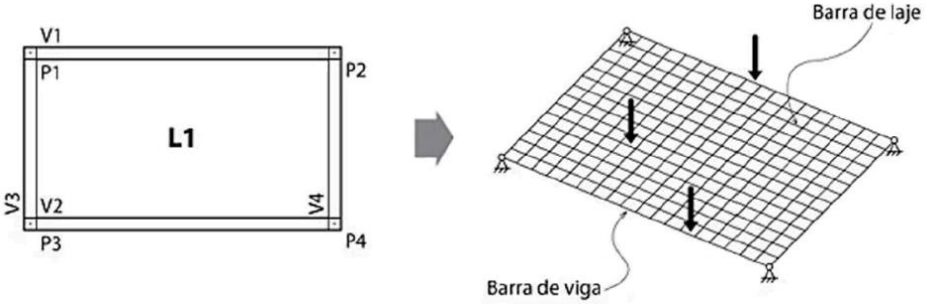

Fig. 1. Beam grid and slab [2].

International Journal of Current Science Research and Review
ISSN: 2581-8341
Volume 06 Issue 12 December 2023
DOI: 10.47191/ijcsrr/V6-i12-99, Impact Factor: 6.789
IJCSRR @ 2023
www.ijcsrr.org

The model consists in discretizing the slab into bars positioned normally in the primary and secondary directions (Fig. 1), making each bar represent a section of the slab, creating a virtual equivalent model. The bars that compose the grid must be divided into an appropriate number of strips, depending on the geometry and dimensions of the floor. Usually, a bar spacing of 50 cm is used, except in regions with a high concentration of efforts, where in these cases a more refined analysis is required [2]. This greater discretization of bars is done to evaluate whether eventual stress peaks correspond to the behavior expected by the engineer in the structural analysis since these errors are inherent to the grid model.

Also, according to Kimura [2], after the application of vertical loads, the distribution of efforts in the slabs and beams is performed automatically through the stiffness of each bar. Fontes [12] mentions that "the slabs can be satisfactorily modeled as a mesh of bars, with bending stiffness and torsional stiffness referring to the strips of slabs represented by them".

The existing nodes at the intersections of the bars have three degrees of freedom, one translation, and two rotations, being possible to obtain the vertical displacements, shear force, bending moment, and torsion efforts. Through the grid model, it is not possible to analyze the horizontal actions acting on a structure [2]. This occurs once the premise for a grid model is that the loads are applied perpendicularly to the plane, and the horizontal actions are contemplated in the space frame model.

2.2.2 Space frame

According to Kimura [2], currently the space frame model is one of the most used for the analysis and design of structures with computational aid. The model consists of three-dimensional analysis of the building (Fig. 2), allowing a complete and efficient evaluation of the global behavior of the structure. This model is composed of bars that represent the beams and pillars, allowing for the simultaneous application of vertical and horizontal loads on the structure.

The justification for the representation of beams and pillars as bar elements is due to the concept shown in item 14.4.1 of ABNT NBR 6118 [4], where these elements have a length greater than three times the largest dimension of the cross-section. Thus, according to their structural function, they receive the designations of beams, pillars, ties, and arches.

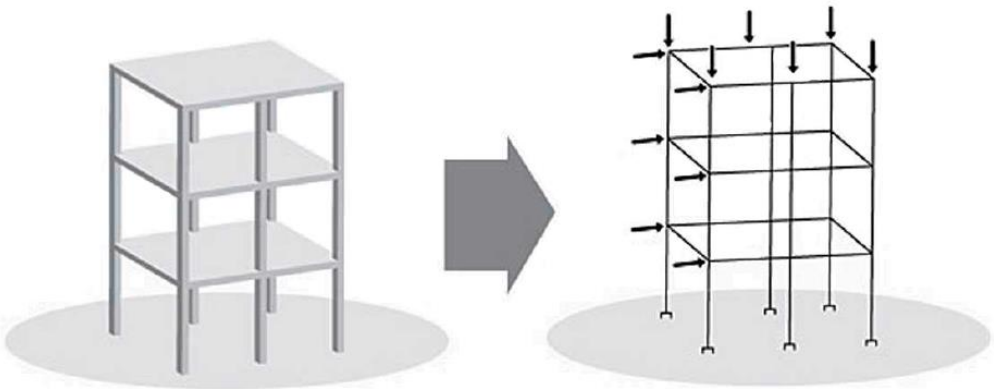

Fig. 2. Space frame [2].

Because of the three-dimensional analysis in the space frame model, each bar intersection has six degrees of freedom, and it is possible to obtain displacements, normal forces, shear, bending moment, and torsion. The intersections between beam and column bars can be rigid, semi-rigid, or flexible.

According to Kimura [2], in this model, the slabs are not used because they are elements that have high stiffness in the horizontal plane, capable of making the structure's behavior compatible in an equivalent manner at all points of the floor. The effect of the slabs on the space frame is designated as a rigid diagram and can be considered through approximate models.

One of the models used, according to Corrêa [13], is to admit that the floor of a structure works as an element with infinite stiffness in its plane, where the floor starts to work as a rigid diagram, distributing the horizontal actions among the bracing structures. In the TQS system, the rigid diagram effect is simulated approximately, through the lateral stiffening of the beams [14].

Another method is through the consideration of nodes with infinite dimensions in the connections between beams and pillars in the formation of aporticated structures. Item 14.6.2.1 of ABNT NBR 6118 [4] recommends that the sections of linear elements belonging to the region common to the intersection of two or more elements can be considered rigid, i.e., nodes with finite dimensions, as illustrated in Fig. 3.

International Journal of Current Science Research and Review
ISSN: 2581-8341
Volume 06 Issue 12 December 2023
DOI: 10.47191/ijcsrr/V6-i12-99, Impact Factor: 6.789
IJCSRR @ 2023
www.ijcsrr.org

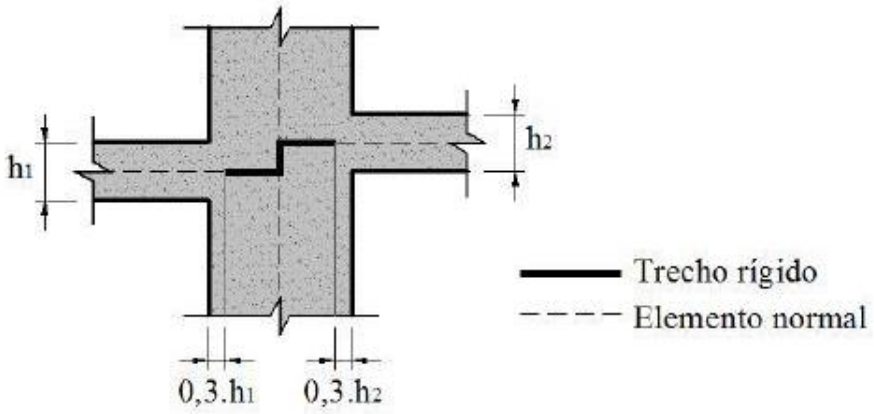

Fig. 3. Rigid sections [15].

In the TQS system, the distribution of loads of the slabs on the space frame beams is performed by transferring the reactions of the slab bars present in the grid model [16]. This structural analysis order is contemplated in model IV of the software.

2.2.3 Integrated model

The integrated model consists of a structural analysis through a single body, formed by a space frame composed of elements that simulate the slabs, beams, and pillars, as shown in Fig. 4. Through this model, the bar meshes of the slabs are inserted into the space frame, allowing better compatibility of deformations in all structural elements after the application of stresses [14].

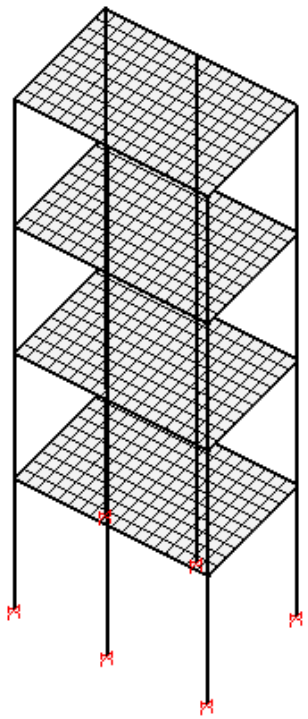

Fig. 4. - Space frame with beams grids and slabs [14].

Through the integrated model, it is possible to simultaneously apply vertical and horizontal forces on the building. Each node of the structure has six degrees of freedom, being possible to obtain displacements, normal forces, shear, bending moment, and torsion. The presence of the slabs in the space frame means that they are considered in the global stability analysis of the

International Journal of Current Science Research and Review
ISSN: 2581-8341
Volume 06 Issue 12 December 2023
DOI: 10.47191/ijcsrr/V6-i12-99, Impact Factor: 6.789
IJCSRR @ 2023
www.ijcsrr.org

building. In addition, the model allows the calculation of shrinkage and temperature forces in structural elements [17]. In TQS software, this model is implemented in the so-called "model VI" of structural analysis.

2.3 Nonlinearity in reinforced concrete structures

The effects of nonlinearity in a building can be understood as a disproportionate response of the structure due to the acting loads. According to Vasconcelos, 1985 *apud* CARMO [7], "in the stability study may arise cases in which the ruin by loss of stability occurs with loads far away from the elastic regime. In these cases, the calculations made in the elastic regime can provide results against safety".

In the analysis of a reinforced concrete structure, the effects of nonlinearity must be considered, caused basically by the change in material properties, called physical nonlinearity, and by the geometric change in the structure, designated geometric nonlinearity.

2.3.1 Physical nonlinearity

The physical nonlinearity in a reinforced concrete structure is related to the behavior of the materials when subjected to acting loads. Concrete and steel do not present a linear behavior, changing their properties as the loads are applied. It is possible to see this behavior through the concrete stress-strain diagram shown in Fig. 5.

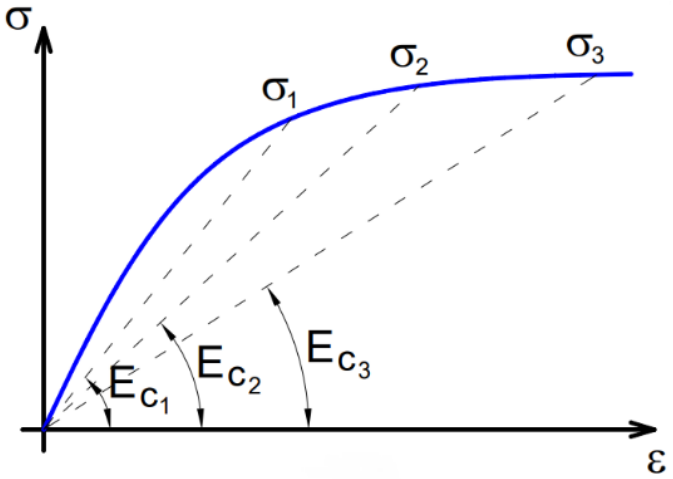

Fig. 5. Stress-strain diagram of concrete [3].

Cracking in concrete due to tensile stresses is another important factor in the analysis of physical nonlinearity in structures. One of the methods used to consider physical nonlinearity in reinforced concrete structures is by reducing the stiffness of structural elements [2].

According to ABNT NBR 6118 [4], "for the analysis of second order global efforts, in reticulated structures with at least four floors, physical nonlinearity can be considered approximately, taking the following values as the stiffness of the structural elements:"

- Slabs: $(EI)_{sec} = 0{,}3E_{ci}I_c$
- Beams: $(EI)_{sec} = 0{,}4\ E_{ci}I_c$ to $As' \neq As$
  $(EI)_{sec} = 0{,}5\ E_{ci}I_c$ to $As' = As$
- Pillars: $(EI)_{sec} = 0{,}8E_{ci}I_c$

where:

E_{ci} – tangent modulus of elasticity;

I_c – the moment of inertia of the gross concrete section, including, when applicable, the collaborating tables.

International Journal of Current Science Research and Review
ISSN: 2581-8341
Volume 06 Issue 12 December 2023
DOI: 10.47191/ijcsrr/V6-i12-99, Impact Factor: 6.789
IJCSRR @ 2023
www.ijcsrr.org

2.3.2 Geometric nonlinearity

In a simplified way, it can be said that the effects due to geometric nonlinearity in reinforced concrete structures are caused by the equilibrium in the deformed condition as the loads are applied. Such effects can be determined through an analysis of the structure in its final equilibrium position [18]. It is possible to make an analogy of the geometric nonlinearity of a structure, through the application of a horizontal and vertical force on the top of a vertical bar clamped at its base.

When the bar is being analyzed in the equilibrium position, i.e., when it has not yet been displaced, vertical, horizontal, and bending moment reactions arise at its base. As the bar moves from its original position, there is an increase in bending moment until it reaches its equilibrium position and the stress increases are negligible, as illustrated in Fig. 6.

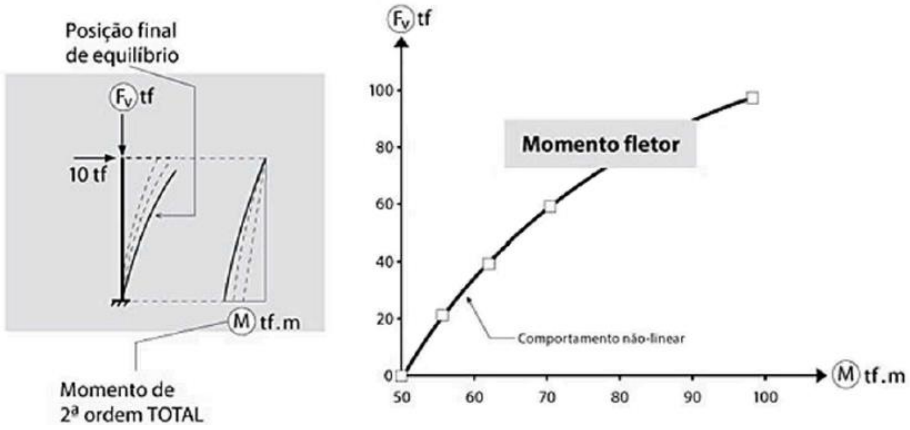

Fig. 6. Effects of geometric nonlinearity [2].

In practice, often the effects caused by geometric nonlinearity cause significant stress increases. The consideration of the effects of geometric nonlinearity is fundamental in the analysis of the global stability of reinforced concrete buildings [2].

2.4 Global stability of structures

The evaluation of the global stability of a building is one of the most important stages of structural analysis, where it aims to ensure safety in the face of loss of capacity to resist increases in stresses and strains, due to horizontal and vertical actions acting on a structure [19].

2.4.1 Second-order effects in structures

The effects in structures due to the performance of vertical and horizontal loads when it is in their initial position, i.e., when their geometry has not yet presented deformations, are called first-order effects. The effects generated in the structure when analyzed in the deformed position are called second-order effects [2].

According to ABNT NBR 6118 [4], second-order effects can be classified as global, local, and localized. The global effects are caused by the displacement of structures due to the joint action of vertical and horizontal loads. The local effects occur in an isolated way in structural elements, influencing the efforts along their length. The localized effects occur in specific regions of a structural element, generating an increase in stress in the region.

Also, according to ABNT NBR 6118 [4], a structure is classified as a fixed node structure when the second-order effects are less than 10% of the first-order effects. The mobile node structures are those in which the actions caused by the second-order effects are greater than 10% of the first-order effects, in which case it is mandatory to consider the global, local, and localized second-order effects.

2.4.2 Parameters for global stability assessment of buildings

Global stability analysis in buildings must be performed in all structural projects. The study of global stability aims to classify a structure according to its lateral displacement, arising from horizontal displacements, due to vertical loads in a building [20].

International Journal of Current Science Research and Review
ISSN: 2581-8341
Volume 06 Issue 12 December 2023
DOI: 10.47191/ijcsrr/V6-i12-99, Impact Factor: 6.789
IJCSRR @ 2023
www.ijcsrr.org

2.4.2.1 Deflection/height ratio (a/H)

According to Oliveira [21], the deflection/height ratio is one of the oldest methods used to evaluate the stability and behavior of a building, and it can be defined by the ratio between the maximum lateral deflection by the total height of the building. This method is used to verify the limit state of excessive deformations and is usually proposed in absolute value or through the fraction of the span considered [7].

Besides checking the total displacement of the building, it is also necessary to analyze the displacements between floors. According to ABNT NBR 6118 [4], the maximum horizontal displacement allowed at the top of the building is H/1700, where H is the total height of the building. For the displacement between floors, the allowable limit is H/850, where in this case, H is the height between floors.

2.4.2.2 Parameter α

Developed by Beck and König in 1966, the α stability parameter seeks to evaluate the possibility of dispensing the second-order effects acting on a structure. The model consists of a column clamped at its base and free at the top, with a constant section along its length and with material presenting an elastic-linear behavior [22].

Through the model cited above, in 1991, Franco and Vasconcelos used the stiffness of the bracing elements of a structure to evaluate the global stability of buildings. Thus, through Equation 1 it is possible to determine the α parameter and estimate the global stability of a building.

$$\alpha = H \cdot \sqrt{\frac{N_k}{EI_{eq}}} \quad (1)$$

where:
H – total building height, measured from the top of the foundation;
N_k – the sum of the vertical loads acting on the structure;
EI_{eq} – stiffness modulus of the building's brace structures, equivalent to a constant section pillar, set at the base and free at the top.

One of the methods used to determine the equivalent stiffness is through the association of bracing systems that act in the same direction of a structure (Fig. 7). The analysis is performed by determining the displacement at the top of a building, subject to a uniformly distributed load along its length.

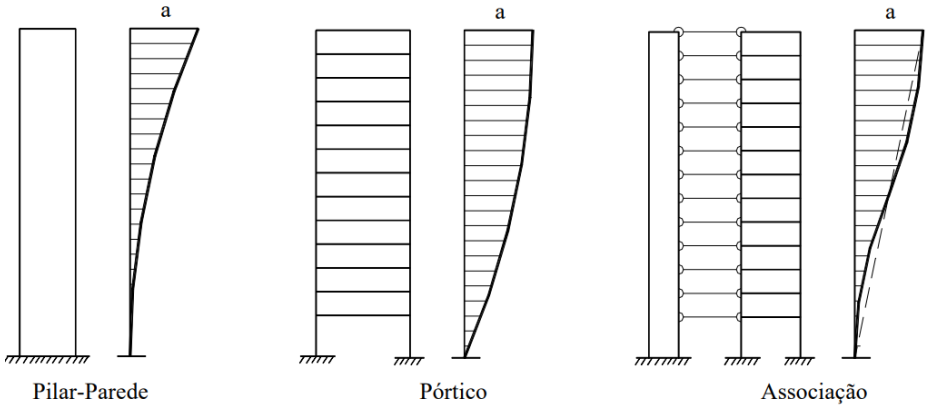

Fig. 7. Association of bracing systems [23].

According to Aufieri [22], the association of bracing systems that act in the same direction of a structure is only possible through the high stiffness of the slabs, which work as labeled bars at their ends, joining a system to the other. Through the displacement obtained at the top of the structure after load application, it is possible to determine the equivalent stiffness of the structure through the following equation:

International Journal of Current Science Research and Review
ISSN: 2581-8341
Volume 06 Issue 12 December 2023
DOI: 10.47191/ijcsrr/V6-i12-99, Impact Factor: 6.789
IJCSRR @ 2023
www.ijcsrr.org

$$EI_{eq} = \frac{q \,.\, H^4}{8 \,.\, a_k} \qquad (2)$$

where:
q – distributed loading;
H – total building height;
a_k – horizontal displacement at the top of the structure.

According to ABNT NBR 6118 [4], for a structure to be considered as fixed nodes and second-order effects can be disregarded in the design, the α parameter must be less than α1. Otherwise, the structure is classified as a mobile node structure, and second-order effects must be considered in structural design.

$\alpha_1 = 0{,}2 + 0{,}1n$ if: $n \leq 3$
$\alpha_1 = 0{,}6$ if: $n \geq 4$

where:
n – number of floors above the foundation.

Also, according to ABNT NBR 6118 [4], the value of α1 = 0.6 applied to structures with four or more floors is used only for usual reinforced concrete buildings, with other values indicated for certain types of structures. In the case of structures formed only by frames, the value of α1 = 0.5 is adopted. For structures with column-wall associations and frames associated with column walls, the value of α1 = 0.6 is adopted. For structures with bracing consisting exclusively of wall pillars, the value of α1 = 0.7 is adopted.

2.4.2.3 Coefficient γz

Developed by Brazilians Mario Franco and Augusto Vasconcelos in 1991, the γz parameter is another method for evaluating the global stability of a building. Unlike the α parameter, which only allows estimating the need or not for second-order effects in structural calculations, the γz coefficient allows first-order efforts to be increased, thus obtaining the final efforts simply and efficiently. According to item 15.7.2 of ABNT NBR 6118 [4], it is possible to estimate the final design efforts by increasing the first-order horizontal efforts by 0.95.γz, and this process is valid only for $\gamma z \leq 1.3$.

The process to determine the γz coefficient starts from a first-order analysis, where the structure subjected to horizontal loads in its initial position generates first-order moments at its base. As the horizontal loads cause displacements in the structure, the vertical actions end up generating an increase in bending moments, called second-order moments. This process occurs numerous times until these increases are negligible (Fig. 8) and equilibrium occurs in the case of stable structures [18].

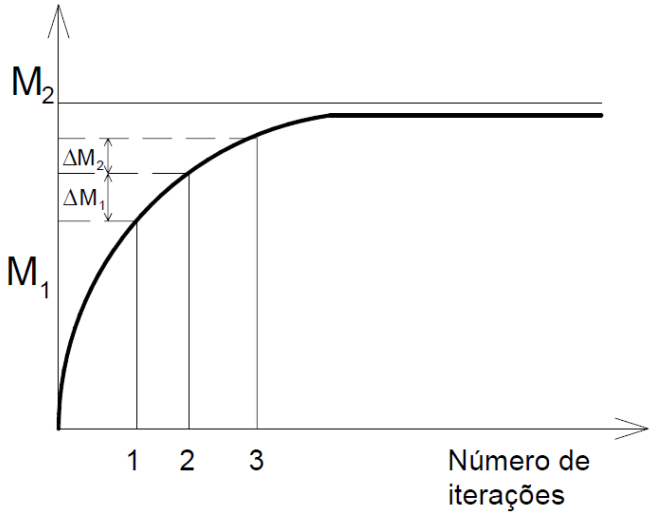

Fig. 8. Determination of the final moment [1].

International Journal of Current Science Research and Review
ISSN: 2581-8341
Volume 06 Issue 12 December 2023
DOI: 10.47191/ijcsrr/V6-i12-99, Impact Factor: 6.789
IJCSRR @ 2023
www.ijcsrr.org

According to ABNT NBR 6118 [4], the coefficient γz is valid for reticulated structures of at least four floors, determined through the following equation:

$$\gamma_z = \frac{1}{1 - \frac{\Delta M_{tot,d}}{M_{1,tot,d}}} \quad (3)$$

where:

$M_{1,tot,d}$ – the overturning moment, that is, the sum of the moments of all horizontal forces of the combination considered, with their design values, relative to the base of the structure;

$\Delta M_{tot,d}$ – the sum of the products of all vertical forces acting on the structure, in the considered combination, with their design values, by the horizontal displacements of their respective points of application, obtained from the 1st order analysis.

2.4.2.4 Process P-Δ

The P-delta process consists in a geometric nonlinear analysis, which relates the vertical loads with the horizontal displacements, to obtain the final design efforts, considering the second-order effects. According to Lopes, Santos, and Souza, 2005 *apud* MONCAYO [3], "P-delta is an effect that occurs in any structure where the elements are subjected to axial forces, in other words, forces in the longitudinal direction of the part".

Several methods use the P-delta process to determine the second-order efforts in a structure. In this paper, emphasis will be placed on the fictitious lateral load method, also known as the iterative method.

The calculation method consists of an iterative process, where a first-order analysis is initially performed, obtaining the displacements due to the horizontal loads acting on the structure. These displacements are used together with the vertical loads to calculate an increment of equivalent horizontal loads, which are combined with the initial loads at each level of the structure, and new displacements are obtained. This process is repeated several times, as shown in Fig. 9 until the structure reaches an equilibrium position [24].

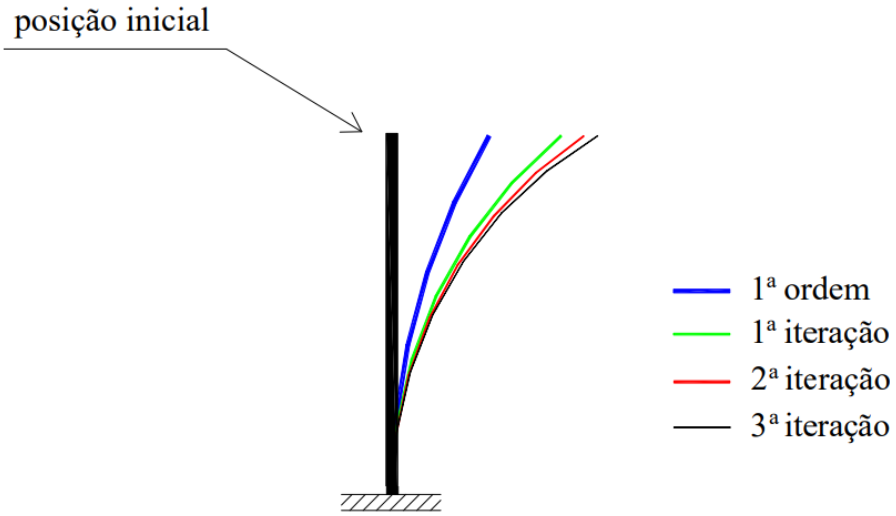

Fig. 9. Position shifted in successive interactions [23].

According to Lima, 2001 *apud* MACGREGOR [23], "the process can be interrupted when the displacements of a given iteration do not exceed in more than 5% those of the previous iteration." After the end of iterations, when the structure presents an equilibrium position, it is possible to obtain the final calculation efforts that will be used in structural design, including second order efforts.

International Journal of Current Science Research and Review
ISSN: 2581-8341
Volume 06 Issue 12 December 2023
DOI: 10.47191/ijcsrr/V6-i12-99, Impact Factor: 6.789
IJCSRR @ 2023
www.ijcsrr.org

3. MATERIALS AND METHODS

The TQS system was used for modeling and analysis of the structure. The software is used to prepare structural projects in reinforced concrete, where its system has resources that allow the engineer to perform an integrated design, analysis, dimensioning, and detailing of reinforced concrete structures [25].

The software allows performing the structural calculation through the grid models of beams and slabs associated with the space frame (model IV), as well as the integrated model (model VI). In addition, the program meets the normative requirements established by ABNT NBR 6118:2014 - Design of concrete structures: procedures [4].

3.1 Preparation of the architectural project

For the development of the research, a hypothetical architectural design of a residential building with one ground floor plus 25 standard floors were prepared. The standard floor consists of four identical apartments per floor, a central core with two elevators and a staircase. On the upper part of the building are located the machine room and the upper reservoir.

The building has a basic architecture, where each apartment consists of two bedrooms, a bathroom, a living room, a kitchen, and a service area. The floor area of the building is about 28 meters long and 14 meters wide, with a total area of 387 sqm, three meters between floors, total height of 83.5 meters, and walls between 20 and 25 cm thick. The isometric view and the floor plan of the standard floor are presented respectively in Figures 10 and 11.

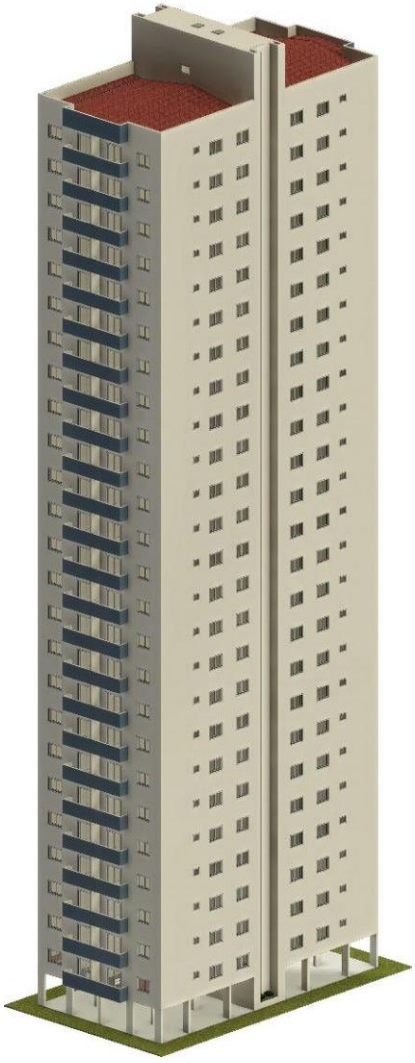

Fig. 10. Isometric view.

International Journal of Current Science Research and Review
ISSN: 2581-8341
Volume 06 Issue 12 December 2023
DOI: 10.47191/ijcsrr/V6-i12-99, Impact Factor: 6.789
IJCSRR @ 2023
www.ijcsrr.org

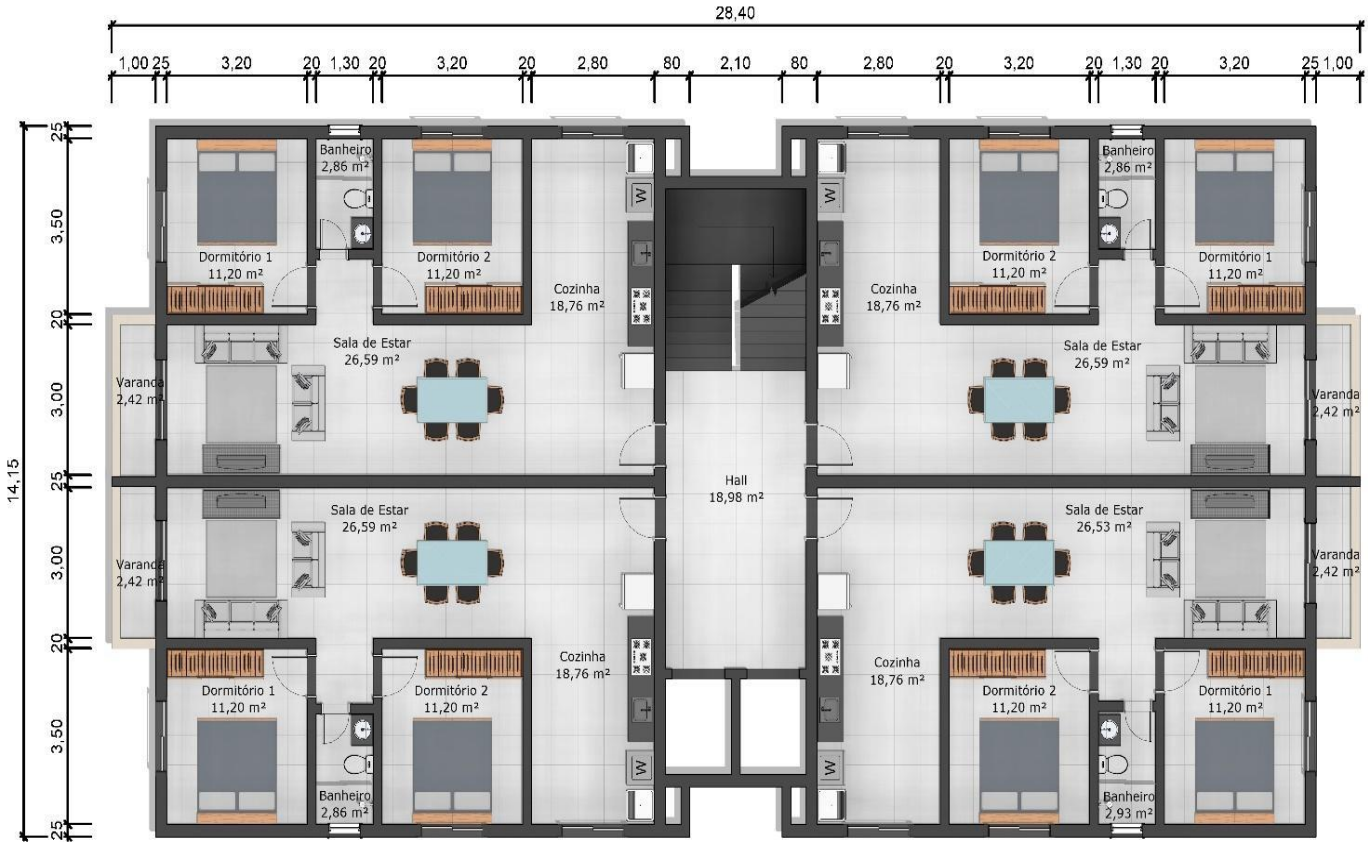

Fig. 11 – Ground plan of the standard floor.

3.2 Structural conception

The first step in the structural design was placing the pillars at a distance between 3 and 5 meters, aligned uniformly forming frames with the beams. In addition, to improve the absorption of horizontal forces in the areas of the stairs and elevators, pillars with greater rigidity were positioned. To analyze the global stability of the building, two different structural conceptions were performed, presented below:

- Case A

In case A, the beams were launch aligned with the walls of the upper floor, with dimensions of 20x60 cm and 15x40 cm. The adopted slabs were of the massive type, with a thickness of 8 centimeters. Emphasizing that is the minimum thickness that can be used for solid floor slabs not in balance, according to item 13.2.4.1 of ABNT NBR 6118 [4]. The pillars have a rectangular section and were positioned to stiffen the structure in the direction of lower inertia. The floor plan of the standard floor for case A is presented in Fig. 12.

International Journal of Current Science Research and Review
ISSN: 2581-8341
Volume 06 Issue 12 December 2023
DOI: 10.47191/ijcsrr/V6-i12-99, Impact Factor: 6.789
IJCSRR @ 2023
www.ijcsrr.org

Fig. 12. Floor plan of the typical floor - case A.

- Case B

For case B, the internal beams were removed and only the beams at the ends of the building were used. The wall loads were applied directly on the solid slab with a thickness of 16 cm, which is the minimum thickness that can be used for these slabs according to item 13.2.4.1 of ABNT NBR 6118 [4]. The cross-sections of the pillars were kept the same as the previous design. The floor plan of the standard floor for case B is shown in Fig. 13.

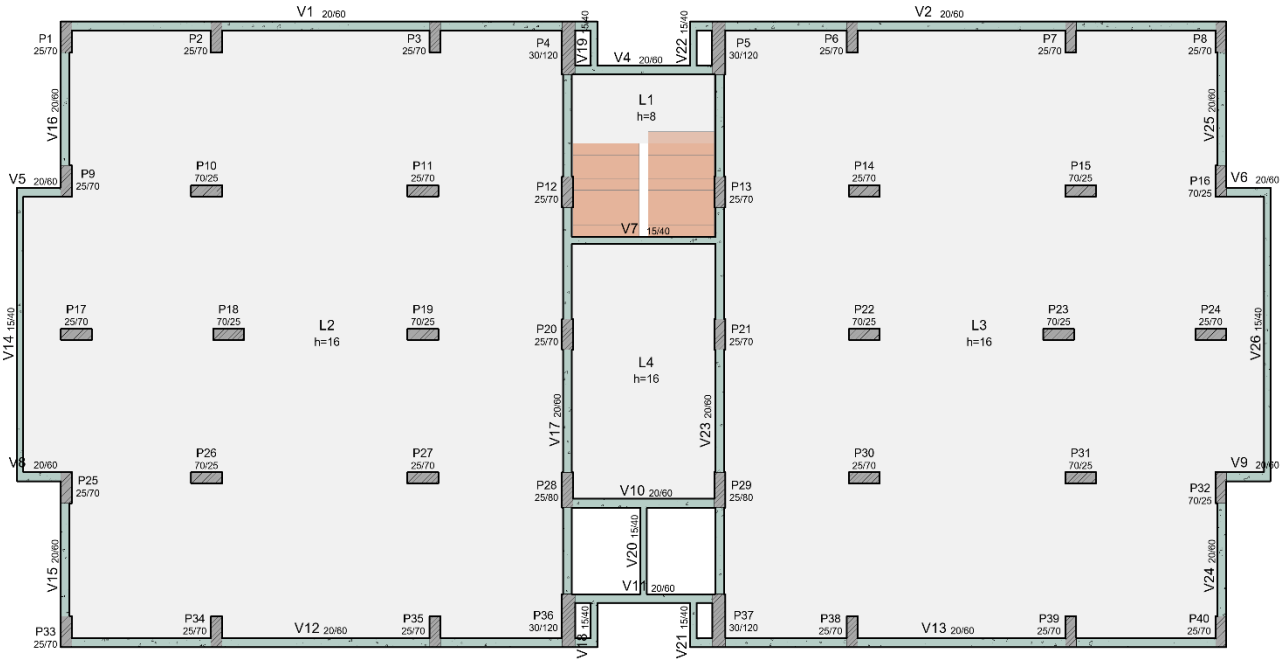

Fig. 13. Floor plan of the typical floor - case B.

International Journal of Current Science Research and Review
ISSN: 2581-8341
Volume 06 Issue 12 December 2023
DOI: 10.47191/ijcsrr/V6-i12-99, Impact Factor: 6.789
IJCSRR @ 2023
www.ijcsrr.org

3.3 Definition of materials and actuating actions

Using ABNT NBR 6118 [4], the environmental aggressiveness class was defined as moderate, i.e., class II. Through the definition of the environmental aggressiveness class, the reinforcement coverings of the structural elements were defined, being adopted as 3 cm for the beams and pillars and 2.5 cm for the slabs. The characteristic strength of the concrete was defined in 35 MPa and the CA-50 steel was adopted for the structure in general and CA-60 for the stirrups. It is worth mentioning that the adoption of a compressive strength higher than the minimum for environmental aggressiveness class II can be justified by the dimensions of the building and the magnitude of the compressive stresses in the pillars, also helping in the global stability of the building.

The loads adopted for the structural calculation were obtained from ABNT NBR 6120 [26], such as the specific weight of the reinforced concrete which was 25 KN/m³, and the specific weight of the hollow ceramic block walls, which was 12 KN/m³. For the facing loads of the solid slabs, the value of 1 KN/m² was adopted, while the variable loads used to calculate the slabs of the bedrooms, bathroom, living room, and kitchen were 1.5 KN/m², for the corridors and stairs for common use, 3 KN/m² was adopted, and 1 KN/m² for all roof slabs with access only for maintenance or inspection.

The wind loads were calculated automatically by the TQS system, according to the guidelines proposed by ABNT NBR 6123 [10]. For the calculation of wind loads, the following information related to the building and terrain location were inserted:

- Base wind speed = 30 m/s;
- Topographical factor (S1) = 1.00;
- Terrain roughness (S2) = category III;
- Building dimensions (S2) = class C;
- Static factor (S3) = 1.00.

3.4 Characteristics of the mathematical model

In this work, the real stiffness of the supports was not considered through the incorporation of elastic supports in the model; this situation would generate an efforts' change presented in the structural elements as well as in the reactions of the foundations. The structures were analyzed considering the models with stiffened supports. In addition, the soil-structure interaction was not considered for the study.

4. RESULTS AND DISCUSSIONS

The analysis of the results for the stability parameters was performed according to the directions of the wind loads acting on the building, exemplified by Fig. 14.

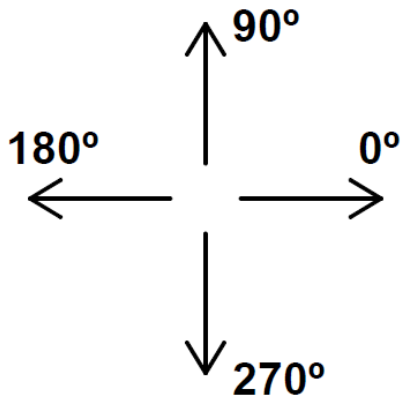

Fig. 14. Directions of wind action [3].

4.1 Case A

The results obtained for the stability parameters α, γz, P-Δ and displacements for the beam grid and slab model associated with the space frame model, as well as for the integrated model are presented in Tab. 1.

International Journal of Current Science Research and Review
ISSN: 2581-8341
Volume 06 Issue 12 December 2023
DOI: 10.47191/ijcsrr/V6-i12-99, Impact Factor: 6.789
IJCSRR @ 2023
www.ijcsrr.org

Tab. 1. Stability parameters for case A.

	Angle	*Model Grids*	*Integrated Model*	*Variation (%)*	
Parameter α	0° - 180°	0,648	0,633	-2,31	
	90° - 270°	0,657	0,658	0,15	
Coefficient γz	0° - 180°	1,090	1,085	-0,46	
	90° - 270°	1,083	1,084	0,09	
Process P-Δ	0°	1,085	1,085	0,00	
	90°	1,084	1,087	0,28	
	180°	1,101	1,088	-1,18	***Maximum Displacement (cm)***
	270°	1,084	1,083	-0,09	
Total Displacement	0° - 180°	0,76	0,74	-2,63	4,91
	90° - 270°	1,92	1,92	0,00	
Displacement between floors	0° - 180°	0,04	0,04	0,00	0,35
	90° - 270°	0,09	0,09	0,00	

For the α parameter, all results were higher than the limit of 0.6 established by ABNT NBR 6118 [4] for fixed node structures. The results obtained for both models showed similar results for the 90° and 270° directions, and a small variation in the 0° and 180° directions. According to Lima [23], although the α parameter works as a good indicator of the structure stiffness, its use for building stability analysis can provide very conservative results. This occurs because the parameter is very simplified, making it often necessary to use another parameter to obtain the second-order efforts.

In the analysis of the γz coefficient, all situations presented values lower than 1.10, and then, the structure was classified as fixed nodes according to ABNT NBR 6118 [4]. As with the α parameter, the results obtained for the γz coefficient presented similar values for both models in the 90° and 270° directions, and a small variation in the 0° and 180° directions.

The variation between the models for the directions of 0° and 180° is due to the lower stiffness of the structure in that direction, where the presence of the slabs in the integrated model cause greater stiffness to the building, thus generating a reduction in stability parameters. The minimum difference in the 90° and 270° directions is due to pillar positions, causing greater stiffness to the structure in that direction so the slabs have little influence on the stability of the building.

In the P-Δ process, the results were similar in both directions and models. However, for the grids model in the 180° direction, the second-order effects were greater than 10% of the first-order effects, unlike the occurred in the analysis of the γz coefficient. Finally, the displacements between pavements and total did not indicate significant differences between the models, and all situations indicated results lower than the limit defined by ABNT NBR 6118 [4].

The maximum allowable displacements were obtained through Table 13.3 of ABNT NBR 6118 [4]. The standard recommends that the limits to be considered for effects on non-structural elements caused, for example, due to lateral movement of the building, caused by wind action, should be analyzed through the frequent combination, with $\psi 1 = 0.3$. Highlighting that both displacements should not be used as stability parameters, being advisable to use them only to evaluate the limits state of excessive deformations [21].

Despite the difference in the results obtained between the models, there is no major interference to the overall stability of the building. According to TQS Informática [14], this occurs mainly in structures where stability is ensured by the presence of beam and column frames, and where the slabs have a minor influence on the stability of the building. Moreover, according to Bueno [1], the major responsibility for the stability of a structure are the frames formed by beams and pillars, and although the slabs have a large stiffness in their plan, they have little influence on global stability.

To verify the relationship of the stability parameters previously obtained with the forces generated in the pillars, a bending moment check was performed at the base of the pillars of two frames of the building, shown in Fig. 15.

International Journal of Current Science Research and Review
ISSN: 2581-8341
Volume 06 Issue 12 December 2023
DOI: 10.47191/ijcsrr/V6-i12-99, Impact Factor: 6.789
IJCSRR @ 2023
www.ijcsrr.org

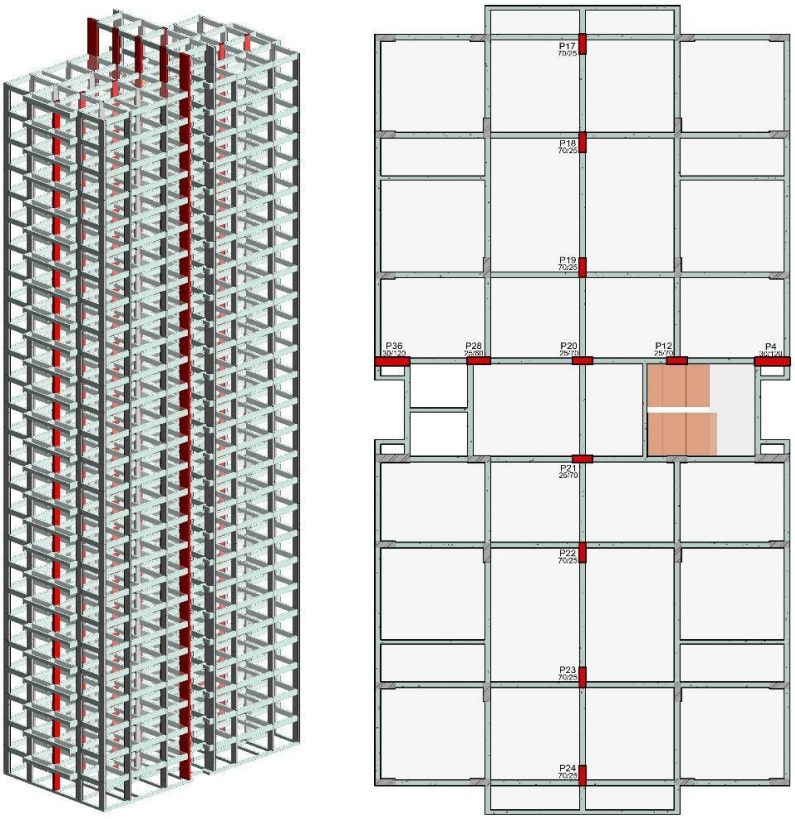

Fig. 16. Identification of the analyzed pillars.

The figure 16 shows the bending moment obtained at the base of pillar 17 for wind action in the 0° direction, for both models studied.

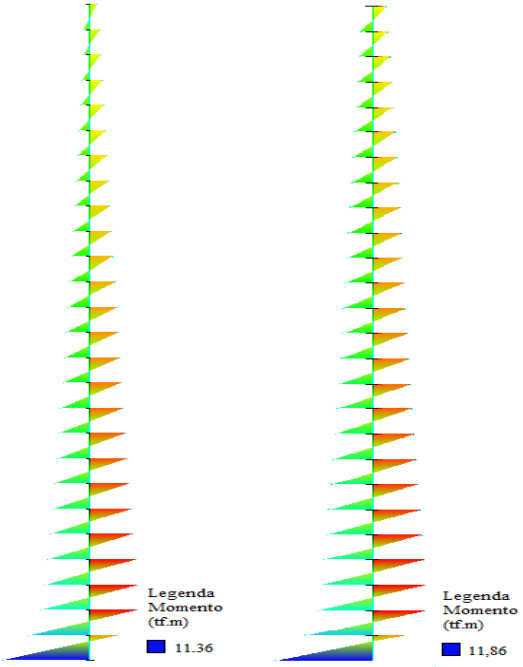

Fig. 16. Example of the bending moment obtained at the base of pillar P17.

International Journal of Current Science Research and Review
ISSN: 2581-8341
Volume 06 Issue 12 December 2023
DOI: 10.47191/ijcsrr/V6-i12-99, Impact Factor: 6.789
IJCSRR @ 2023
www.ijcsrr.org

The results obtained for the other pillars are presented as a function of the wind action on the structure in Tables 2 and 3.

Tab. 2. Bending moment at the base of the pillars of frame 1 - Case A

Pillar	*Direction*	*Bending moment (tf.m)*		*Variation (%)*	*Pillar*	*Direction*	*Bending moment (tf.m)*		*Variation (%)*
		Model Grids	Integrated Model				Model Grids	Integrated Model	
P17	0°	11,36	11,86	4,40	**P21**	0°	2,01	2,1	4,48
	90°	-2,92	-3,1	6,16		90°	18,31	18,71	2,18
	180°	-11,29	-10,34	-8,41		180°	-2,16	-1,97	-8,80
	270°	3,14	3,05	-2,87		270°	-18,76	-18,54	-1,17
P18	0°	11,35	11,88	4,67	**P22**	0°	11,21	11,72	4,55
	90°	-2,78	-2,87	3,24		90°	-2,84	-2,82	-0,70
	180°	-13,39	-12,36	-7,69		180°	-13,03	-11,98	-8,06
	270°	2,95	2,81	-4,75		270°	2,87	2,82	-1,74
P19	0°	11,45	12,01	4,89	**P23**	0°	11,78	12,36	4,92
	90°	-2,79	-2,86	2,51		90°	-2,88	-2,85	-1,04
	180°	-12,79	-11,68	-8,68		180°	-12,95	-11,88	-8,26
	270°	2,92	2,79	-4,45		270°	2,85	2,82	-1,05
P20	0°	1,89	1,97	4,23	**P24**	0°	10,13	10,65	5,13
	90°	18,19	18,78	3,24		90°	-3,07	-3,12	1,63
	180°	-2,28	-2,09	-8,33		180°	-12,54	-11,58	-7,66
	270°	-18,87	-18,47	-2,12		270°	3,00	3,07	2,33

Tab. 3. Bending moment at the base of frame 2 pillars - Case A

Pillar	*Direction*	*Bending moment (tf.m)*		*Variation (%)*
		Model Grids	Integrated Model	
P4	0°	4,84	4,91	1,45
	90°	81,48	85,02	4,34
	180°	-6,17	-6,38	3,40
	270°	-83,99	-81,03	-3,52
P12	0°	1,73	1,88	8,67
	90°	18,86	19,5	3,39
	180°	-2,01	-1,79	-10,95
	270°	-18,48	-17,91	-3,08
P20	0°	1,89	1,97	4,23
	90°	18,19	18,78	3,24
	180°	-2,28	-2,09	-8,33
	270°	-18,87	-18,47	-2,12
P28	0°	2,17	2,25	3,69
	90°	25,8	26,57	2,98
	180°	-2,54	-2,37	-6,69
	270°	-27,08	-26,5	-2,14
P36	0°	4,73	4,89	3,38
	90°	81,72	84,11	2,92
	180°	-5,49	-5,13	-6,56
	270°	-84,65	-82,59	-2,43

International Journal of Current Science Research and Review
ISSN: 2581-8341
Volume 06 Issue 12 December 2023
DOI: 10.47191/ijcsrr/V6-i12-99, Impact Factor: 6.789
IJCSRR @ 2023
www.ijcsrr.org

Through the results, it is noticed that the grid model in relation to the integrated model presented a small variation of the bending moment. For both frames analyzed, some of the pillars showed a reduction of the moment, while others showed an increase, with an average variation of 4.5%. Furthermore, the column that presented the greatest variation between the models was column 12, with a variation of 10.95% for wind action in the 180° direction. Therefore, as expected due to the results obtained previously for the stability parameters, the pillars did not present significant variations in bending moment between the models analyzed.

4.2 Case B

The results obtained for the stability parameters and displacements for both models studied are presented in Tab. 4.

Tab. 4. Stability parameters for case B.

	Angle	*Model Grids*	*Integrated Model*	*Variation (%)*	
Parameter α	0° - 180°	1,273	1,024	-19,56	
	90° - 270°	0,890	0,804	-9,66	
Coefficient γz	0° - 180°	1,453	1,258	-13,42	
	90° - 270°	1,158	1,128	-2,59	
Process P-Δ	0°	1,475	1,275	-13,56	
	90°	1,159	1,133	-2,24	
	180°	1,468	1,255	-14,51	***Maximum Displacement (cm)***
	270°	1,158	1,125	-2,85	
Total Displacement	0° - 180°	3,03	1,54	-49,17	4,91
	90° - 270°	3,17	2,41	-23,97	
Displacement between floors	0° - 180°	0,17	0,09	-47,06	0,35
	90° - 270°	0,15	0,11	-26,67	

For case B, the α parameter showed high values for both models and directions, with results well above the limit of 0.6 established by ABNT NBR 6118 [4] for fixed node structures. The results obtained in the analysis between the models indicated a reduction around 19.5% for the 0° and 180° directions, and 9.6% for the 90° and 270° directions of the integrated model concerning the grid model associated with the space frame.

The results obtained for the γz coefficient in the 0° and 180° directions for the grid model associated with the space frame, indicated values above the limit allowed for an approximate consideration of global second-order efforts, i.e., $\gamma z > 1.3$. The integrated model presented for γz and P-Δ a reduction of around 13.5% for the directions 0° and 180°, and 2.5% for the directions 90° and 270° about the grid model associated with the space frame.

It was possible to notice in case B a greater reduction of stability parameters for all directions, but especially for the directions of 0° and 180°. This reduction occurred due to the removal of the internal beams of the building, where the slabs began to have a greater influence on global stability, especially for the directions that have lower stiffness.

For both models and directions, displacements lower than the limits established by standard were obtained. It is worth noting the significant reduction in total displacement, where the integrated model showed a reduction of around 49% for the directions of 0° and 180°, and 24% in the directions of 90° and 270° concerning the grid model. The inter-floor displacement also showed significant results, where the integrated model proved a reduction of around 47% for the 0° and 180° directions, and 27% in the 90° and 270° directions in relation to the grid model.

The integrated model presented a significant reduction in all parameters of the grid model associated with the space frame. This occurs because, according to Bueno [1], in cases of buildings with a mushroom slab or flat slabs, the stiffness of the building is responsibility of the pillars and the slabs have a greater influence on global stability. Thus, the integrated model becomes the most suitable for analysis of buildings with flat slabs, because these will have greater participation in the structure's equilibrium [3].

A comparative analysis of the bending moment at the base of each column of the frames mentioned above was also performed for case B, for both models studied. The results are presented as a function of the wind action on the structure.

International Journal of Current Science Research and Review
ISSN: 2581-8341
Volume 06 Issue 12 December 2023
DOI: 10.47191/ijcsrr/V6-i12-99, Impact Factor: 6.789
IJCSRR @ 2023
www.ijcsrr.org

Through the results presented in Tab. 5 it is possible to see that for wind action in the directions of 0° and 180°, all pillars showed an average reduction of the bending moment of 22.5% of the integrated model relative to the grid model associated with the space frame. For the 90° and 270° directions, all pillars showed an average increase of 11.7%, except pillars 20 and 21, which for all wind directions showed an average reduction of the bending moment of 11.3%.

Tab. 5. Bending moments at the base of pillars of frame 1 - Case B.

Pillar	*Direction*	*Bending moment (tf.m)*		*Variation (%)*	*Pillar*	*Direction*	*Bending moment (tf.m)*		*Variation (%)*
		Model Grids	**Integrated Model**				**Model Grids**	**Integrated Model**	
P17	0°	-23,90	-18,31	-23,39	**P21**	0°	2,91	2,6	-10,65
	90°	2,21	2,58	16,74		90°	24,19	22,66	-6,32
	180°	23,38	17,3	-26,01		180°	-2,83	-2,37	-16,25
	270°	-2,27	-2,53	11,45		270°	-24,42	-22,22	-9,01
P18	0°	23,30	17,93	-23,05	**P22**	0°	23,92	18,05	-24,54
	90°	-2,31	-2,62	13,42		90°	-2,36	-2,63	11,44
	180°	-24,06	-18,17	-24,48		180°	-24,57	-18,2	-25,93
	270°	2,37	2,56	8,02		270°	2,35	2,61	11,06
P19	0°	24,46	18,62	-23,88	**P23**	0°	24,39	18,8	-22,92
	90°	-2,34	-2,62	11,97		90°	-2,35	-2,62	11,49
	180°	-24,12	-17,51	-27,40		180°	-23,88	-17,39	-27,18
	270°	2,38	2,56	7,56		270°	2,32	2,59	11,64
P20	0°	2,85	2,44	-14,39	**P24**	0°	-23,77	-17,86	-24,86
	90°	24,13	22,54	-6,59		90°	2,28	2,57	12,72
	180°	-2,89	-2,37	-17,99		180°	24,49	17,76	-27,48
	270°	-24,5	-22,17	-9,51		270°	-2,25	-2,53	12,44

Through the results presented in Tab. 6 it is possible to see a reduction in the bending moment for all pillars of frame number 2, with an average reduction of 22.6% for the 0° and 180° directions, and 8.4% for the 90° and 270° directions.

Tab. 6. Bending moment at the base of pillars of frame 2 - Case B.

Pillar	*Direction*	*Bending moment (tf.m)*		*Variation (%)*
		Model Grids	**Integrated Model**	
P4	0°	13,38	9,7	-27,50
	90°	108,22	100,98	-6,69
	180°	-13,86	-10,94	-21,07
	270°	-109,52	-97,05	-11,39
P12	0°	2,92	2,45	-16,10
	90°	24,86	23,13	-6,96
	180°	-2,89	-2,19	-24,22
	270°	-24,29	-21,65	-10,87
P20	0°	2,85	2,44	-14,39
	90°	24,13	22,54	-6,59
	180°	-2,89	-2,37	-17,99
	270°	-24,5	-22,17	-9,51

International Journal of Current Science Research and Review
ISSN: 2581-8341
Volume 06 Issue 12 December 2023
DOI: 10.47191/ijcsrr/V6-i12-99, Impact Factor: 6.789
IJCSRR @ 2023
www.ijcsrr.org

P28	0°	4,91	3,71	-24,44
	90°	34,16	31,88	-6,67
	180°	-5,1	-3,8	-25,49
	270°	-35,03	-31,7	-9,51
P36	0°	12,93	9,46	-26,84
	90°	107,11	100,03	-6,61
	180°	-13,04	-9,36	-28,22
	270°	-108,43	-98,28	-9,36

As occurred in the analysis of stability parameters, it was also possible to note a reduction in the values between the models studied for the bending moment at the base of the pillars of the frames analyzed. All pillars showed a significant reduction in the bending moment for the 0° and 180° directions. This occurs due to the greater variation of stability parameters obtained for these directions.

For the wind loads in the 90° and 270° directions, moment increases were obtained for some pillars of frame 1 and a reduction for all pillars of frame 2, but with minor variations when compared with those obtained in the other directions. Despite the increase in bending moment on some pillars of frame 1, it is possible to realize that the wind action for the 90° and 270° directions generate lower forces on these pillars, therefore the increases generated have low influence on their behavior.

4.3 Case A vs. Case B - Beam grid and slab model plus space frame

A comparison between both models of the building under study was performed using the grid model associated with the space frame. The results are shown in Tab. 7.

Tab. 7. Stability parameters - Space frame and grid model.

	Angle	***Case A***	***Case B***	***Variation (%)***	
Parameter α	0° - 180°	0,648	1,273	96,45	
	90° - 270°	0,657	0,890	35,46	
Coefficient γz	0° - 180°	1,090	1,453	33,30	
	90° - 270°	1,083	1,158	6,93	
Process P-Δ	0°	1,085	1,475	35,94	
	90°	1,084	1,159	6,92	
	180°	1,101	1,468	33,33	***Maximum Displacement (cm)***
	270°	1,084	1,158	6,83	
Total Displacement	0° - 180°	0,76	3,03	298,68	4,91
	90° - 270°	1,92	3,17	65,10	
Displacement between floors	0° - 180°	0,04	0,17	325	0,35
	90° - 270°	0,09	0,15	66,67	

From case A to case B, all stability parameters showed significant increases in their values. The α parameter showed an increase of around 96% for the 0° and 180° directions, and 35% in the 90° and 270° directions. The γz coefficient showed an increase of about 33% for the 0° and 180° directions, and 7% in the 90° and 270° directions.

Through the P-Δ process, the results showed an increase of around 35% in the 0° and 180° directions, and 7% in the 90° and 270° directions. Finally, the displacements between pavements and total showed an increase of 325% and 300% respectively for the 0° and 180° directions, and about 66% for the 90° and 270° directions.

It was possible to notice that after the removal of the internal beams (case A to case B), the structure presented a greater lateral displacement, especially in the directions of 0° and 180°. This occurs because, according to Fusco [27], the beams present a

International Journal of Current Science Research and Review
ISSN: 2581-8341
Volume 06 Issue 12 December 2023
DOI: 10.47191/ijcsrr/V6-i12-99, Impact Factor: 6.789
IJCSRR @ 2023
www.ijcsrr.org

considerable contribution to the global stability of buildings. Moreover, according to Alves and Feitosa [28], structural systems without the use of beams present significant disadvantages regarding the stiffness of horizontal displacements of the structure.

A comparative analysis between cases A and B was also performed for the bending moment at the base of the pillars, through the grid model associated with the space frame. As in the previous analyses, the results are presented as a function of the wind action on the building.

The results presented in Tab. 8 show a significant increase in the moments at the base of the pillars of frame 1. For wind action in the 0° and 180° directions, all pillars had an average increase of 86.3% of the bending moment. For the 90° and 270° directions, all pillars showed an average reduction of 20.5%, except pillars 20 and 21, which for all wind directions showed an average increase of 34.8% of the bending moment.

Tab. 8. Bending moment at the base of the pillars of frame 1 - Grid model and space frame.

Pillar	*Direction*	*Bending moment (tf.m)*		*Variation (%)*	*Pillar*	*Direction*	*Bending moment (tf.m)*		*Variation (%)*
		Case A	**Case B**				**Case A**	**Case B**	
P17	0°	11,36	-23,90	110,39	**P21**	0°	2,01	2,91	44,78
	90°	-2,92	2,21	-24,32		90°	18,31	24,19	32,11
	180°	-11,29	23,38	107,09		180°	-2,16	-2,83	31,02
	270°	3,14	-2,27	-27,71		270°	-18,76	-24,42	30,17
P18	0°	11,35	23,30	105,29	**P22**	0°	11,21	23,92	113,38
	90°	-2,78	-2,31	-16,91		90°	-2,84	-2,36	-16,90
	180°	-13,39	-24,06	79,69		180°	-13,03	-24,57	88,56
	270°	2,95	2,37	-19,66		270°	2,87	2,35	-18,12
P19	0°	11,45	24,46	113,62	**P23**	0°	11,78	24,39	107,05
	90°	-2,79	-2,34	-16,13		90°	-2,88	-2,35	-18,40
	180°	-12,79	-24,12	88,58		180°	-12,95	-23,88	84,40
	270°	2,92	2,38	-18,49		270°	2,85	2,32	-18,60
P20	0°	1,89	2,85	50,79	**P24**	0°	10,13	-23,77	134,65
	90°	18,19	24,13	32,66		90°	-3,07	2,28	-25,73
	180°	-2,28	-2,89	26,75		180°	-12,54	24,49	95,30
	270°	-18,87	-24,5	29,84		270°	3,00	-2,25	-25,00

The results presented in Tab. 9 for the pillars of frame 2 show a significant increase in the bending moment at the base of all pillars for both wind directions. From case A to case B, all pillars showed an average increase of the bending moment of 67%, where it was possible to observe a greater variation for the 0° and 180° directions. This occurred due to the greater variation of stability parameters for these directions.

Tab. 9. Bending moment at the base of the pillars of frame 2 - Grid and space frame model.

Pillar	*Direction*	*Bending moment (tf.m)*		*Variation (%)*
		Case A	**Case B**	
P4	0°	4,84	13,38	176,45
	90°	81,48	108,22	32,82
	180°	-6,17	-13,86	124,64
	270°	-83,99	-109,52	30,40
P12	0°	1,73	2,92	68,79
	90°	18,86	24,86	31,81

International Journal of Current Science Research and Review
ISSN: 2581-8341
Volume 06 Issue 12 December 2023
DOI: 10.47191/ijcsrr/V6-i12-99, Impact Factor: 6.789
IJCSRR @ 2023
www.ijcsrr.org

	180°	-2,01	-2,89	43,78
	270°	-18,48	-24,29	31,44
P20	0°	1,89	2,85	50,79
	90°	18,19	24,13	32,66
	180°	-2,28	-2,89	26,75
	270°	-18,87	-24,5	29,84
P28	0°	2,17	4,91	126,27
	90°	25,8	34,16	32,40
	180°	-2,54	-5,1	100,79
	270°	-27,08	-35,03	29,36
P36	0°	4,73	12,93	173,36
	90°	81,72	107,11	31,07
	180°	-5,49	-13,04	137,52
	270°	-84,65	-108,43	28,09

As was also expected due to the results obtained in the analysis of the stability parameters, all pillars showed a significant increase in bending moment at their base, except for some pillars of frame 1 for wind action in the 90° and 270° directions.

4.4 Case A vs. Case B - Integrated Model

A comparison of the two modeling approaches was also performed using the integrated model for the building under study. The results are presented in Tab. 10.

Tab. 10. Stability Parameters - Integrated Model.

	Angle	*Case A*	*Case B*	*Variation (%)*	
Parameter α	0° - 180°	0,633	1,024	61,77	
	90° - 270°	0,658	0,804	22,19	
Coefficient γz	0° - 180°	1,085	1,258	15,94	
	90° - 270°	1,084	1,128	4,06	
Process P-Δ	0°	1,085	1,275	17,51	
	90°	1,087	1,133	4,23	
	180°	1,088	1,255	15,35	***Maximum Displacement (cm)***
	270°	1,083	1,125	3,88	
Total Displacement	0° - 180°	0,74	1,54	108,11	4,91
	90° - 270°	1,92	2,41	25,52	
Displacement between floors	0° - 180°	0,04	0,09	125	0,35
	90° - 270°	0,09	0,11	22,22	

Through the analysis between cases A and B employing the integrated model, it was possible to notice for the α parameter an increase of around 62% for the 0° and 180° directions, and 22% in the 90° and 270° directions. The coefficient γz and P-Δ showed similar results, resulting in an increase of about 16% in the 0° and 180° directions, and 4% in the 90° and 270° directions.

The total and between pavements displacements presented respectively an increase of 108% and 125% for the 0° and 180° directions, and around 24% for the 90° and 270° directions. As in the grid model analysis, through the integrated model it was also possible to notice a significant increase in the lateral displacement of the structure after the removal of the internal beams.

Finally, a comparative analysis between cases A and B was also performed, verifying the efforts in the pillars through the integrated model. The results for frames 1 and 2 are presented in Tables 11 and 12, respectively.

International Journal of Current Science Research and Review
ISSN: 2581-8341
Volume 06 Issue 12 December 2023
DOI: 10.47191/ijcsrr/V6-i12-99, Impact Factor: 6.789
IJCSRR @ 2023
www.ijcsrr.org

Tab. 11. Bending moment at the base of the pillars of frame 1 - Integrated model.

Pillar	*Direction*	*Bending moment (tf.m)*		*Variation (%)*	*Pillar*	*Direction*	*Bending moment (tf.m)*		*Variation (%)*
		Case A	**Case B**				**Caso A**	**Caso B**	
P17	0°	11,86	-18,31	54,38	**P21**	0°	2,1	2,6	23,81
	90°	-3,1	2,58	-16,77		90°	18,71	22,66	21,11
	180°	-10,34	17,3	67,31		180°	-1,97	-2,37	20,30
	270°	3,05	-2,53	-17,05		270°	-18,54	-22,22	19,85
P18	0°	11,88	17,93	50,93	**P22**	0°	11,72	18,05	54,01
	90°	-2,87	-2,62	-8,71		90°	-2,82	-2,63	-6,74
	180°	-12,36	-18,17	47,01		180°	-11,98	-18,2	51,92
	270°	2,81	2,56	-8,90		270°	2,82	2,61	-7,45
P19	0°	12,01	18,62	55,04	**P23**	0°	12,36	18,8	52,10
	90°	-2,86	-2,62	-8,39		90°	-2,85	-2,62	-8,07
	180°	-11,68	-17,51	49,91		180°	-11,88	-17,39	46,38
	270°	2,79	2,56	-8,24		270°	2,82	2,59	-8,16
P20	0°	1,97	2,44	23,86	**P24**	0°	10,65	-17,86	67,70
	90°	18,78	22,54	20,02		90°	-3,12	2,57	-17,63
	180°	-2,09	-2,37	13,40		180°	-11,58	17,76	53,37
	270°	-18,47	-22,17	20,03		270°	3,07	-2,53	-17,59

Tab. 12. Bending moment at the base of the pillars of frame 2 - Integrated model.

Pillar	*Direction*	*Bending moment (tf.m)*		*Variation (%)*
		Case A	**Case B**	
P4	0°	4,91	9,7	97,56
	90°	85,02	100,98	18,77
	180°	-6,38	-10,94	71,47
	270°	-81,03	-97,05	19,77
P12	0°	1,88	2,45	30,32
	90°	19,5	23,13	18,62
	180°	-1,79	-2,19	22,35
	270°	-17,91	-21,65	20,88
P20	0°	1,97	2,44	23,86
	90°	18,78	22,54	20,02
	180°	-2,09	-2,37	13,40
	270°	-18,47	-22,17	20,03
P28	0°	2,25	3,71	64,89
	90°	26,57	31,88	19,98
	180°	-2,37	-3,8	60,34
	270°	-26,5	-31,7	19,62
P36	0°	4,89	9,46	93,46
	90°	84,11	100,03	18,93
	180°	-5,13	-9,36	82,46
	270°	-82,59	-98,28	19,00

International Journal of Current Science Research and Review
ISSN: 2581-8341
Volume 06 Issue 12 December 2023
DOI: 10.47191/ijcsrr/V6-i12-99, Impact Factor: 6.789
IJCSRR @ 2023
www.ijcsrr.org

The results obtained between cases A and B for the integrated model were similar to the previous analysis for the grid model associated with the space frame. In frame 1, all the pillars for wind action in the 0° and 180° directions presented an average increase of the bending moment of 45.7% and, for the 90° and 270° directions, an average reduction of 11%, except for pillars 20 and 21 that for all wind directions presented an average increase of 20.3%. As for frame 2, in all wind directions, the pillars showed an average increase of 37.8%, with greater variations in the directions of 0° and 180°.

Therefore, as in the analysis using the grid model, it was also possible to notice the influence of the beams on the forces generated in the pillars using the integrated model. However, through the results, it is possible to see a reduction in the percentages obtained through the integrated model in comparison to the grid model. Such variations are also observed between cases A and B in the analysis of stability parameters for the models previously studied.

5. CONCLUSIONS

By using the TQS software, this paper conducted a comparative analysis of the global stability parameters, using two different models of a reinforced concrete residential building, through the structural model of beam grid and slabs associated with the space frame, as well as the integrated model.

The results obtained through the first design pointed out that both models presented stability parameters similar to each other. As mentioned earlier, this occurs in structures that have well-defined frames of beams and pillars, causing the slabs to have little influence on the overall stability of the building. It can therefore be concluded that for structures with these characteristics, the beam grid and slab model associated with the spatial frame shows similar results to the integrated model. Thus, the grid model associated with the space frame becomes more suitable, because it will provide greater time savings to the design engineer during the structural processing of the building.

In the second design, the results showed a greater discrepancy between the models studied. Unlike case A, where the stability was guaranteed basically by frames formed by beams and pillars, in case B, the slabs had a greater influence on the overall stability of the building. Therefore, the grid model of beams and slabs associated with the space frame proved less efficient for the stability analysis of buildings with flat slabs, while the integrated model showed better results in the analysis of global stability.

Finally, a comparative analysis between the two structural models was performed. The results showed that regardless of the model used, the beams have a considerable contribution to the global stability of the building, significantly reducing its lateral displacement. According to Alves and Feitosa [28], in these buildings, it can be used rigid cores located normally in the stairwells and elevator shafts, because they have high stiffness and together with the other pillars ensure the overall stability of the building. Therefore, for buildings with flat slabs without the use of beams or only edge beams, pillars with higher stiffness will be necessary, because these will be the main responsible for the overall stability of the building

REFERENCES

1. BUENO, M. M. E. Avaliação dos parâmetros de instabilidade global em estruturas de concreto armado. 2009. 105 f. Dissertação (Mestre em Estruturas e Construção Civil) – Faculdade de Tecnologia, Universidade de Brasília, Brasília, 2009.
2. KIMURA, A. Informática aplicada a estruturas de concreto armado. 2. ed. São Paulo: Oficina de Textos, 2018.
3. MONCAYO, W. J. Z. Análise de segunda ordem global em edifícios com estrutura de concreto armado. 2011. 221 f. Dissertação (Mestre em Ciências) – Escola de Engenharia de São Carlos, Universidade de São Paulo, São Carlos, 2011.
4. ASSOCIAÇÃO BRASILEIRA DE NORMAS TÉCNICAS. NBR 6118: Projeto de estruturas de concreto - Procedimento. Rio de Janeiro. 2014.
5. ASSOCIAÇÃO BRASILEIRA DE NORMAS TÉCNICAS. NBR 8681: Ações e segurança nas estruturas - Procedimento. Rio de Janeiro. 2003.
6. ARAÚJO, J. M. Curso de concreto armado. 3. ed. v. 1. Rio Grande: Dunas, 2010.
7. CARMO, R. M. S. Efeitos de segunda ordem em edifícios usuais de concreto armado. 1995. 135 f. Dissertação (Mestre em Engenharia de Estruturas) – Escola de Engenharia de São Carlos, Universidade de São Paulo, São Carlos, 1995.
8. GONÇALVES, R. M. et al. Ação do vento nas edificações: teoria e exemplos. 1. ed. São Carlos, 2004.
9. GIONCO, J. S. Concreto armado: projeto estrutural de edifícios. São Carlos, 2007.

International Journal of Current Science Research and Review
ISSN: 2581-8341
Volume 06 Issue 12 December 2023
DOI: 10.47191/ijcsrr/V6-i12-99, Impact Factor: 6.789
IJCSRR @ 2023
www.ijcsrr.org

10. ASSOCIAÇÃO BRASILEIRA DE NORMAS TÉCNICAS. NBR 6123: Forças devidas ao vento em edificações. Rio de Janeiro. 1988.
11. MARTHA, L. F. Análise de estruturas: conceitos e métodos básicos. Rio de Janeiro: Elsevier, 2010.
12. FONTES, F. F. Análise estrutural de elementos lineares segundo a NBR 6118:2003. 2005. 137 f. Dissertação (Mestre em Engenharia de Estruturas) – Escola de Engenharia de São Carlos, Universidade de São Paulo, São Carlos, 2005.
13. [13] CORRÊA, M. R. S. Aperfeiçoamento de modelos usualmente empregados no projeto de sistemas estruturais de edifícios. 1991. 342 f. Tese (Doutor em Engenharia Civil) – Escola de Engenharia de São Carlos, Universidade de São Paulo, São Carlos, 1991.
14. Modelo VI. TQS Informática, São Paulo, 2020. Disponível em: <https://www.tqs.com.br/v16/destaques/modelo-vi-projeto-estrutural.html>. Acesso em: 15 jul. 2022.
15. CARAMORI, T. Estudo de trechos rígidos na análise estrutural de edificações em concreto armado. 2017. 98 f. Monografia (Graduação em Engenharia Civil) – Universidade Federal de Santa Maria, Santa Maria, 2017.
16. TQSDocs. TQS Informática, São Paulo, 2020. Disponível em: <https://docs.tqs.com.br/Docs/Details?id=3147&language=pt-BR>. Acesso em: 24 ago. 2022.
17. FRANCESCHI, Lucas. Como optar entre o modelo de análise integrado ou de grelha com pórtico espacial. AltoQi, 2021. Disponível em: <https://suporte.altoqi.com.br/hc/pt-br/articles/360001391833-Como-optar-entre-o-modelo-de-an%C3%A1lise-integrado-ou-de-grelha-com-p%C3%B3rtico-espacial>. Acesso em: 15 jul. de 2022.
18. PINTO, R. S. Não-linearidade física e geométrica no projeto de edifícios usuais de concreto armado. 1997. 130 f. Dissertação (Mestre em Engenharia Civil) – Escola de Engenharia de São Carlos, Universidade de São Paulo, São Carlos, 1997.
19. PAIXÃO, J. F. M.; ALVES, E. C. Análise de estabilidade global em edifícios altos. Revista Eletrônica De Engenharia Civil, Goiânia, v. 13, n. 1, p. 48-63, 2017.
20. CRUZ, J. M. F.; FERREIRA, E. T.; LUCENA, C. A. T. D. A estabilidade global dos edifícios altos. João Pessoa: Leia livros, 2019.
21. OLIVEIRA, J. C. A. Estimativa do índice global de esbeltez de edifícios altos de concreto armado. 1998. 166 f. Dissertação (Mestre em Ciências) – Faculdade de Tecnologia, Universidade de Brasília, Brasília, 1998.
22. AUFIERI, F. A. Diretrizes para o dimensionamento e detalhamento de pilares de edifícios em concreto armado. 1997. 165 f. Dissertação (Mestre em Engenharia de Estruturas) – Escola de Engenharia de São Carlos, Universidade de São Paulo, São Carlos, 1997.
23. LIMA, J. S. Verificações da punção e da estabilidade global em edifícios em concreto: Desenvolvimento e aplicação de recomendações normativas. 2001. 249 f. Dissertação (Mestre em Engenharia de Estruturas) – Escola de Engenharia de São Carlos, Universidade de São Paulo, São Carlos, 2001.
24. IGLESIA, S. M. O efeito P-delta nas estruturas de edifícios. AltoQi, Santa Catarina, 2017.
25. TQSDocs. TQS Informática, São Paulo, 2022. Disponível em: <https://docs.tqs.com.br/Docs/Details?id=3124&language=pt-BR>. Acesso em: 14 jun. 2022.
26. ASSOCIAÇÃO BRASILEIRA DE NORMAS TÉCNICAS. NBR 6120: Ações para o cálculo de estruturas de edificações. Rio de Janeiro. 2019.
27. FUSCO, P. B. Estruturas de concreto: solicitações normais. Rio de Janeiro, Guanabara Dois, 1983.
28. ALVES, E. C.; FEITOSA, L. A. Análise da estabilidade global de edifícios altos em lajes lisas considerando a interação solo-estrutura. Revista IBRACON de estruturas e materiais, Vitória, v. 13, n. 1, p. 183-199, 2020.

Cite this Article: José Pedro Diniz Figueiredo, Leovegildo Douglas Pereira de Souza (2023). Global Stability Study of a Reinforced Concrete Building: Comparison between Grid and Space Frame Model with an Integrated Model. International Journal of Current Science Research and Review, 6(12), 8530-8554